JOURNAL OF VIROLOGY, Nov. 2005, p. 13747–13758 Vol. 79, No. 21
0022-538X/05/$08.00+0 doi:10.1128/JVI.79.21.13747–13758.2005

Brome Mosaic Virus 1a Nucleoside Triphosphatase/Helicase Domain Plays Crucial Roles in Recruiting RNA Replication Templates

Xiaofeng Wang,[1,2] Wai-Ming Lee,[1]‡ Tokiko Watanabe,[1] Michael Schwartz,[1,2]† Michael Janda,[1,2] and Paul Ahlquist[1,2]*

Institute for Molecular Virology[1] and Howard Hughes Medical Institute,[2] University of Wisconsin, Madison, Wisconsin 53706

Received 23 December 2004/Accepted 4 August 2005

Positive-strand RNA virus RNA replication is invariably membrane associated and frequently involves viral proteins with nucleoside triphosphatase (NTPase)/helicase motifs or activities. Brome mosaic virus (BMV) encodes two RNA replication factors: 1a has a C-terminal NTPase/helicase-like domain, and $2a^{pol}$ has a central polymerase domain. 1a accumulates on endoplasmic reticulum membranes, recruits $2a^{pol}$, and induces 50- to 70-nm membrane invaginations (spherules) serving as RNA replication compartments. 1a also recruits BMV replication templates such as genomic RNA3. In the absence of $2a^{pol}$, 1a dramatically stabilizes RNA3 by transferring RNA3 to a membrane-associated, nuclease-resistant state that appears to correspond to the interior of the 1a-induced spherules. Prior results show that the 1a NTPase/helicase-like domain contributes to RNA recruitment. Here, we tested mutations in the conserved helicase motifs of 1a to further define the roles of this domain in RNA template recruitment. All 1a helicase mutations tested showed normal 1a accumulation, localization to perinuclear endoplasmic reticulum membranes, and recruitment of $2a^{pol}$. Most 1a helicase mutants also supported normal spherule formation. Nevertheless, these mutations severely inhibited RNA replication and 1a-induced stabilization of RNA3 in vivo. For such 1a mutants, the membrane-associated RNA3 pool was both reduced and highly susceptible to added nuclease. Thus, 1a recruitment of viral RNA templates to a membrane-associated, nuclease-resistant state requires additional functions beyond forming spherules and recruiting RNA to membranes, and these functions depend on the 1a helicase motifs. The possibility that, similar to some double-stranded RNA viruses, the 1a NTPase/helicase-like domain may be involved in importing viral RNAs into a preformed replication compartment is discussed.

Positive-strand RNA viruses are a large class of viral pathogens causing numerous clinically and economically important diseases of humans, animals, and plants. Although such viruses encompass substantial variation in morphology, genetic organization, host range, and other properties, they all share fundamental similarities in their basic replication mechanisms. For example, genome replication by positive-strand RNA viruses is universally associated with intracellular membranes, which usually are induced by viral replication proteins to form invaginations or vesicles (51). In the early steps of positive-strand RNA virus replication, the viral genomic RNAs first serve as templates for translating these replication proteins and often other viral proteins. Once such proteins induce formation of the membrane-associated replication complexes, the incoming viral genomic RNA must be recruited away from translation to serve as a template for RNA replication. This genomic RNA transition from translation to RNA replication is a crucial step in early infection and must be tightly regulated to effectively balance translation and replication (44). Nevertheless, the mechanisms of selecting and recruiting viral RNAs for replication are not well understood.

One positive-strand RNA virus for which such processes have been studied is brome mosaic virus (BMV), a member of the alphavirus-like superfamily of human, animal, and plant viruses. The BMV genome is composed of three RNAs. RNA1 and RNA2 encode replication proteins 1a (109 kDa) and $2a^{pol}$ (94 kDa), respectively. 1a has an N-terminal domain with enzymatic activities required for capping viral RNA and a C-terminal superfamily I nucleoside triphosphatase (NTPase)/helicase-like (NTPase/hel) domain (2, 3, 30, 34). $2a^{pol}$ possesses a central polymerase-like domain and an N-terminal region that binds the 1a NTPase/hel domain (7, 27, 45). RNA3 encodes the 3a protein, required for cell-to-cell movement in plants (4, 42), and coat protein.

Yeast (*Saccharomyces cerevisiae*) cells expressing 1a and $2a^{pol}$ support BMV RNA replication, in which negative- and positive-strand RNA3 and subgenomic RNA4 are produced and amplified using DNA-transcribed RNA3 as the original template (24). This yeast system duplicates the features of BMV RNA replication in natural host plants, including proper intracellular localization; dependence on 1a, $2a^{pol}$, and specific *cis*-acting signals; and production of excess positive-strand over negative-strand RNA (52, 54). In addition, yeast support selective encapsidation of BMV RNAs (33).

1a is a key player in BMV RNA replication (7, 25, 52). In yeast expressing 1a alone, 1a is associated with perinuclear endoplasmic reticulum (ER) membranes and induces formation of compartments, or spherules, in which BMV RNA replication occurs (9, 49, 52). These spherules are 50- to 70-nm invaginations of the outer perinuclear ER membrane into the

* Corresponding author. Mailing address: Institute for Molecular Virology, University of Wisconsin-Madison, 1525 Linden Dr., Madison, WI 53706-1576. Phone: (608) 263-5916. Fax: (608) 265-9214. E-mail: ahlquist@wisc.edu.

† Present address: Department of Biological Sciences, Vanderbilt University, Nashville, TN 37235.

‡ Present address: Department of Pediatrics, University of Wisconsin, Madison, WI 53792.

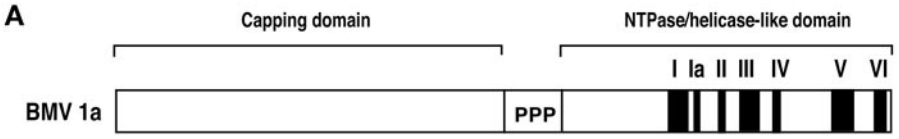

B

motif	aa position	sequence	mutant(s) tested
I	683-692	MVDGVAGCG**K**T	K691A
II	752-758	LLV**D**EAG	D755A
III	781-791	G**D**TE**Q**IS**F**K**SR**	G781S
			Q785A, Q785E
			F788A
			S790A, S790W
			R791A
IV	808-815	DVVHK**TYR**	TY813AA
			R815L
V	899-913	IKTV**H**EAQGISVDNV	H903A
VI	934-941	VALT**R**HKK	R938A

C

B. s.	**Pcr A helicase**	**250**	GDAD**Q**SI**Y**R**WR** **260**
E. coli	**Rep helicase**	**241**	GDDD**Q**SIYHWR **251**
BMV	**1a**	**781**	**G**DTE**Q**IS**F**K **SR** **791**

FIG. 1. (A) Schematic of BMV 1a protein. 1a contains an N-terminal capping domain (aa 1 to 515) with m7G-methyltransferase and m7GMP binding activities and a C-terminal NTPase/helicase-like domain (aa 562 to 961) containing seven conserved signature helicase motifs (black boxes). A proline-rich region (PPP) separates the two domains. (B) Sequences of signature helicase motifs and mutants tested in this work. Sequences of six motifs (I to VI) were identified based on the criteria of Gorbalenya and Koonin (17). Amino acids shown in boldface were mutated as indicated at the right. (C) Comparison of motif III from *B. stearothermophilus* PcrA, *E. coli* Rep, and BMV 1a. Shaded amino acids are identical in all three proteins. The effects of mutations at the amino acids shown in boldface have been studied previously for PcrA helicase. Amino acids in BMV 1a that appear in boldface type and underlined were examined in this work.

ER lumen, with interiors that are connected to the cytoplasm through a neck (52). Similar membrane invaginations are associated with RNA replication in natural infections by bromoviruses, alphaviruses, nodaviruses, and many other positive-stranded RNA viruses (15, 21, 28, 35, 51, 59). 1a also recruits $2a^{pol}$ to spherules by interacting with the $2a^{pol}$ N terminus (7, 27, 52). In the absence of $2a^{pol}$, 1a recruits RNA3 to a membrane-associated, nuclease-resistant, and detergent-susceptible state in which RNA3 half-life and accumulation increase by 20 to 50 fold and RNA3 translation is inhibited (25, 52). This state appears to correspond to the interior of the 1a-induced spherules, since in yeast cells expressing 1a and $2a^{pol}$ and replicating RNA3, positive- and negative-strand RNA3 templates and nascent RNA are retained in an indistinguishable, membrane-associated, nuclease-resistant state, and immunogold electron microscopy (EM) localizes bromo-UTP-labeled nascent RNA to spherules (52).

Although helicases have traditionally been viewed as NTP-dependent double-stranded (ds) nucleic acid unwinding enzymes, recent data suggest that helicases may also be involved in RNA translocation, modulating RNA-protein interactions, etc. (39, 53, 56). 1a has a C-terminal superfamily I NTPase/hel domain (amino acids [aa] 562 to 961) containing seven helicase signature motifs, denoted I, Ia, and II to VI, with motifs I and II comprising a putative NTPase domain (Fig. 1) (3, 17, 31, 34). Multiple results show that the 1a NTPase/hel domain contributes to the RNA synthesis functions of the assembled replication complex. When preformed RNA replication complexes are shifted to a nonpermissive temperature, a strong temperature-sensitive insertion mutation near the 1a NTPase domain blocks further synthesis of positive- and negative-strand genomic RNAs and subgenomic RNA4 (34). Moreover, studies with other animal and plant-infecting members of the alphavirus superfamily show that conserved NTPase/hel domains paralleling that of BMV 1a have an RNA triphosphatase activity contributing to capping of viral RNA products by removing 5′ γ-phosphates (37, 57). In addition to these roles in RNA synthesis, the 1a NTPase/hel domain has a role(s) in earlier steps of RNA replication complex assembly. In particular, mutations in three of seven 1a helicase motifs block in vivo RNA3 stabilization (2). However, the nature of these contributions is not clear.

To gain more insight into the functions of the 1a NTPase/hel domain and the mechanisms by which 1a induces RNA3 in vivo to become membrane associated and stabilized, we made and tested additional mutations in six of the seven helicase signature motifs. We show here that mutations in each of these signature helicase motifs blocked BMV RNA replication. Most replication-defective mutations allowed spherule formation and readily detectable RNA3 recruitment to membranes but blocked RNA3 from achieving the nuclease-resistant state induced by wild-type (wt) 1a. The data show that the 1a NTPase/hel domain plays crucial roles in recruiting BMV RNA templates into replication complexes.

MATERIALS AND METHODS

Yeast strain and cell growth. Yeast strain YPH500 (*MATα ura3-52 lys2-801 ada2-101 trp1-Δ63 his3-Δ200 leu2-Δ1*) was used in all experiments. Cultures were grown at 30°C in defined synthetic medium containing 2% galactose (GAL) as a carbon source. Leucine, tryptophan, uracil, histidine, or combinations thereof were omitted as required to maintain selection for different plasmids. Cells were grown in GAL medium for two to three passages (24 to 36 h) and harvested when the optical density at 600 nm (OD_{600}) was between 0.4 and 0.8.

Plasmids and plasmid construction. Expression of BMV 1a, $2a^{pol}$, and RNA3 was driven by the *GAL1* promoter, which is galactose inducible and glucose repressible. BMV 1a and 1a mutants were expressed from pB1YT3 (3), a centromeric plasmid with a *URA3* marker, in all experiments unless specified. BMV $2a^{pol}$ and BMV RNA3 were expressed from centromeric plasmids pB2YT5 and pB3MS82 (54) with *LEU2* and *TRP1* markers, respectively. pB3MS82 expresses a BMV RNA3 derivative in which the coat protein gene has a four-nucleotide insertion, abolishing expression of the coat protein (54).

The Sec63p-green fluorescent protein (GFP) fusion protein was expressed from plasmid pWSECG. To construct pWSECG, pJK59 (a gift from P. Silver, Department of Biological Chemistry and Molecular Pharmacology, Harvard University) was digested with SacI and KpnI. The fragment containing the *SEC63* promoter, coding sequence, and GFP open reading frame was inserted into SacI- and KpnI-digested plasmid YCplac22, a centromeric vector with a *TRP1* marker.

Mutants K691A, D755A, and G781S were originally made by T. Ahola (3) with plasmid pB1CT19 (23). The mutations were introduced into pB1YT3 by replacing the wild-type 1a sequence by an MscI-PmeI fragment from pB1CT19, and the mutated sequence of the cloned fragment was confirmed by sequencing.

Point mutations Q785A, Q785E, F788A, S790A, S790W, R791A, TY813AA, R815L, H903A, and R938A were introduced into the BMV 1a coding sequence by PCR-based, site-directed mutagenesis (22). PCR fragments with each of these mutations were digested with SacII and BamHI and cloned to pB1YT3 to replace the corresponding wild-type fragments. After being cloned, all the fragments were sequenced to confirm the presence of the intended point mutations and absence of unintended mutations.

The coding sequence of BMV 1a fragment 1aC, which contains 1a amino acids 424 to 961, was PCR amplified with pB1YT3 as the template. A BamHI site and an XhoI site were introduced into the 5′ and 3′ ends of the PCR fragment. The PCR product was cloned to pGEX-4T-1 (Amersham Biosciences, Piscataway, NJ) to make pGT-1aC and sequenced to make sure that no unintended mutations were present. The same process was applied to each of the 1a helicase mutants to express the corresponding 1a helicase mutant fragments.

Membrane flotation assay. Yeast spheroplasts prepared from 15 OD_{600} units of cells were resuspended in 500 μl lysis buffer (50 mM Tris-HCl [pH 7.4], 5 mM EDTA, 150 mM NaCl, 5 mM benzamidine, 2 mM phenylmethylsulfonyl fluoride [PMSF], and 10 μg/ml [each] aprotinin, leupeptin, and pepstatin A) and lysed with 15 strokes of a Dounce homogenizer. The total lysate was centrifuged for 5 min at 4°C at 500 × *g* to remove cell debris, and 250 μl of the supernatant was mixed with 500 μl of 60% OptiPrep (Axis-Shield, Oslo, Norway). Density gradient centrifugation was performed for 5 h at 55,000 rpm in a Beckman TLS55 rotor using 600 μl of each sample overlaid with 1.4 ml of 30% OptiPrep and 100 μl of lysis buffer (5). After centrifugation, the samples were divided into six fractions from top to bottom of the gradient, boiled in Laemmli loading buffer, and stored at −80°C. Sodium dodecyl sulfate-polyacrylamide gel electrophoresis (SDS-PAGE) and Western blotting were performed using 10 μl of boiled sample from each fraction. The assay was performed at least twice for each mutant.

Cell fractionation assays. For the BMV $2a^{pol}$ recruitment assay, yeast spheroplasts prepared from 5 OD_{600} units of cells were lysed by being pipetted up and down in lysis buffer (50 mM Tris [pH 8.0], 10 mM EDTA, 10 mM dithiothreitol [DTT], 5 mM benzamidine, 2 mM PMSF, and 10 μg [each] of aprotinin, leupeptin, and pepstatin A per ml). Half of the lysate was retained without further treatment to represent total extracted protein. The other half of the lysate was then centrifuged for 5 min at 20,000 × *g* at 4°C. The supernatant was removed and retained, and the pellet was washed once and resuspended in lysis buffer. Equal volumes of the total supernatant and pellet fractions were boiled in Laemmli loading buffer and used in SDS-PAGE and Western blotting.

For the BMV RNA3 cell fractionation assay, yeast spheroplasts prepared from 12 OD_{600} units of cells were lysed in 300 μl lysis buffer (50 mM Tris-Cl [pH 8.0], 2.5 mM EDTA, 1 mM PMSF, 5-μg/ml pepstain, 10-μg/ml leupeptin, 10-μg/ml aprotinin, 10 mM benzamidine). An aliquot of the lysate (50 μl) was removed for total RNA isolation (see below), and 200 μl of lysate was transferred to a new tube and centrifuged for 5 min at 20,000 × *g*. The supernatant was transferred to a new tube, and the pellet was briefly centrifuged to remove remaining supernatant and resuspended in 200 μl of lysis buffer. For RNase treatment, 0.5 U of micrococcal nuclease (MNase) was added to 50 μl of supernatant and pellet fractions, incubated at 30°C for 15 min, and inactivated by addition of 1 μl of 0.5 M EGTA (pH 8.0). Total RNA was extracted using a QIAGEN (Valencia, CA) RNA Easy kit. Equal volumes of RNA preparations from each fraction were used for Northern blotting, and equal loading of total RNA was verified by ethidium bromide staining of rRNA bands. The same blots were hybridized with both BMV RNA3 and yeast 18S rRNA probes. To correct for imperfection in cell fractionation, the percentage of membrane-associated RNA3 was adjusted by subtracting the percentage of 18S rRNA present in the pellet fraction. All fractionation experiments were repeated at least two times, and representative results are shown in the figures.

Expression and purification of glutathione *S*-transferase (GST)-1aC and corresponding 1a helicase mutants. The plasmid pGT-1aC was transformed into *Escherichia coli* strain C41(DE3). An overnight culture was diluted 1:100 in 500 ml 2×YT medium (1.6% yeast extract, 1% tryptone, 0.5% NaCl) with 100 μg/ml ampicillin and grown at 30°C to an OD_{600} of around 1.0. Isopropylthio-β-D galactopyranoside (IPTG) was added to a concentration of 0.1 mM, and cells were harvested 1 h later and frozen at −80°C. The frozen cell pellet was resuspended in 15 ml lysis buffer (1× phosphate-buffered saline, 5 mM DTT, 5% glycerol, and 1 tablet of complete protease inhibitor cocktail from Roche Applied Science, Germany) and sonicated three times for 30 s. Triton X-100 was added to a concentration of 1%, and the cell lysate was kept on ice for 30 min. The lysate was centrifuged at 35,000 × *g* for 25 min at 4°C to yield a supernatant (S35-1) and a pellet (P35). The P35 was resuspended in 15 ml of lysis buffer, sonicated three times, treated with Triton X-100, and centrifuged to yield a supernatant (S35-2) and a pellet. The S35-2 supernatant was mixed with S35-1 and incubated with 1 ml glutathione-Sepharose 4B beads (Amersham Biosciences) at 4°C. The supernatant-beads were loaded onto a 25-ml column (Bio-Rad, Hercules, CA), washed with 30 ml 1× phosphate-buffered saline–5% glycerol, and eluted with 15 mM reduced glutathione–5% glycerol. To each elute fraction, glycerol was added to a final concentration of 15%. The protein concentration of each eluted fraction was determined by the Bradford assay (Bio-Rad). The same procedure was applied to express and purify each of the corresponding 1a helicase mutants.

ATPase assay. ATPase activity was assayed as previously described (37) with minor modifications. Purified proteins were incubated with 5 μCi [α-^{32}P]ATP in 10 μl of 50 mM Tris-HCl (pH 7.4), 5 mM $MgCl_2$, 5 mM DTT, 150 μM ATP, and 20 U of RNAsin (Ambion, Austin, TX) at 37°C for 30 min. Reactions were stopped by adding EDTA to 50 μM, and 1 μl of each reaction mixture was spotted on polyethyleneimine-cellulose thin-layer chromatography (TLC) plates (Fisher Scientific, Pittsburgh, Pa.) and developed with 0.5 M LiCl–0.5 M formic acid. The TLC plate was visualized using a PhosphoImager (Molecular Dynamics, Sunnyvale, CA), and the intensities of ATP and ADP spots were measured. To compare the ATPase activities of wt 1a with the helicase mutants, 1 μg of each protein preparation was used and each ATPase activity assay was performed three times.

Immunofluorescent labeling and confocal microscopy. Yeast cells were fixed and immunostained as described previously (36, 48). Briefly, yeast cells coexpressing either wt or mutant 1a and Sec63-GFP were grown to an OD_{600} value of 0.4 to 0.8, fixed with 5% formaldehyde, spheroplasted with lyticase, and permeabilized with 0.1% Triton X-100. Cells were incubated first with rabbit anti-1a serum at a 1:100 dilution and then with donkey anti-rabbit antibodies conjugated with Texas red at a 1:100 dilution. Images were acquired with a Bio-Rad 1024 double-channel confocal microscope at the W. M. Keck Laboratory for Biological Imaging at the University of Wisconsin—Madison. Experiments were performed at least twice for each sample.

EM. Prior to fixation, yeast cells were treated with lyticase to partially remove cell walls and to release osmotic pressure to facilitate the observation of viral spherules (52). Yeast cell fixation, dehydration, and embedding were performed as previously described (52). Thin sections (each, 70 nm) were placed on copper grids and stained with uranyl acetate and lead citrate. Images were obtained with a Philips CM120 transmission electron microscope at the Medical School Electron Microscopy Facility of the University of Wisconsin—Madison. Spherule diameters were measured with the imaging program analySIS Docu (Soft Imaging Systems, Lakewood, Colo.). For each wt 1a and 1a helicase mutant, 45 to 60 spherules were measured.

RESULTS

Mutations in BMV 1a NTPase/hel domain. The C-terminal half of BMV 1a contains a superfamily I NTPase/hel domain

(amino acids 562 to 961), with all seven conserved signature motifs (I, Ia, and II to VI) (Fig. 1A) (17, 31). Previous work showed that three point mutations (K691A, D755A, and G781S) in motifs I, II, and III, respectively, abolish the ability of 1a to protect BMV RNA3 and to support RNA replication (3). In this work, we tested whether additional mutations at these and other helicase motifs (Fig. 1A) would impair 1a activities and, if they did, whether mutations at differing motifs would affect BMV replication at the same or different steps.

Additional 1a helicase mutations (Fig. 1B) were designed in part by consideration of structure/function results with other well-characterized members of the superfamily I NTPase/hel family, including PcrA, a DNA helicase of *Bacillus stearothermophilus*, and Rep helicase of *E. coli* (6, 11, 32, 58). In particular, based on the crystal structure and mutational analysis of PcrA helicase, motif III residues Y257, W259, and R260 (Fig. 1C) bind to single-stranded DNA (ssDNA), while Q254 directly binds the γ-phosphate of ATP and has been proposed as a γ-phosphate sensor (11, 12, 58). Similarly, in the crystal structure of Rep helicase, equivalent motif III residues Y248, W250, and R251 (Fig. 1C) contact ssDNA (32). Based on alignment of the similar motif III sequences of BMV 1a, PcrA, and Rep (Fig. 1C), we chose 1a residues Q785, F788, S790, and R791 for study (Fig. 1B), because these four amino acids are in corresponding positions and either identical or chemically similar to the above amino acids of PcrA and Rep helicases. Given the functional importance of the corresponding amino acids in PrcA, such mutations would be expected to inhibit helicase or/and NTPase activity.

Arginine residue R287 in motif IV of PcrA contacts the γ-phosphate of ATP (58). An arginine (R815) is also present in the corresponding position of BMV 1a motif IV and was mutated to leucine (Fig. 1B). 1a T813 is conserved in several viral helicases or putative helicases, such as the 126-kDa protein of tobacco mosaic virus and 1a protein of cucumber mosaic virus (1). T813 and Y814 were also present in the consensus sequence of viral (superfamily 1) RNA helicases (pfm01443; National Center for Biotechnology Information conserved domain database) (40), and both were mutated to alanine in a single mutant (TY813AA). Similarly, since a histidine in motif V of PcrA and Rep binds to ssDNA (6, 32), the corresponding H903 from motif V of BMV 1a was mutated to alanine.

A conserved arginine is found in motif VI across all helicase superfamilies (6, 38). In PcrA, the corresponding R610 contacts the γ-phosphate of ATP (58). This so-called arginine finger has been proposed to bridge NTPase activity to helicase activity (6, 38). Accordingly, in BMV 1a, an R938 at the equivalent position in motif VI was mutated to alanine.

Since three 1a sequences between motifs I and II were found to match the recognized features of motif Ia, no mutations were targeted to this motif.

1a helicase mutations block RNA replication. We first checked whether any of the mutations shown in Fig. 1B might destabilize the 1a protein in yeast cells. Western blotting using anti-1a antiserum showed that each mutant 1a protein accumulated 80 to 106% of the 1a wt level in yeast cells expressing a 1a helicase mutant alone, with $2a^{pol}$, RNA3, or both $2a^{pol}$ and RNA3 (Fig. 2A and data not shown). In about half of the experiments, mutants TY813AA(III) (the Roman numeral in parenthesis represents the motif number), R815L(IV), and R938A(VI) were associated with a major breakdown product of ~60 kDa, which reduced full-length 1a levels to 50 to 60% of those of wt 1a (data not shown).

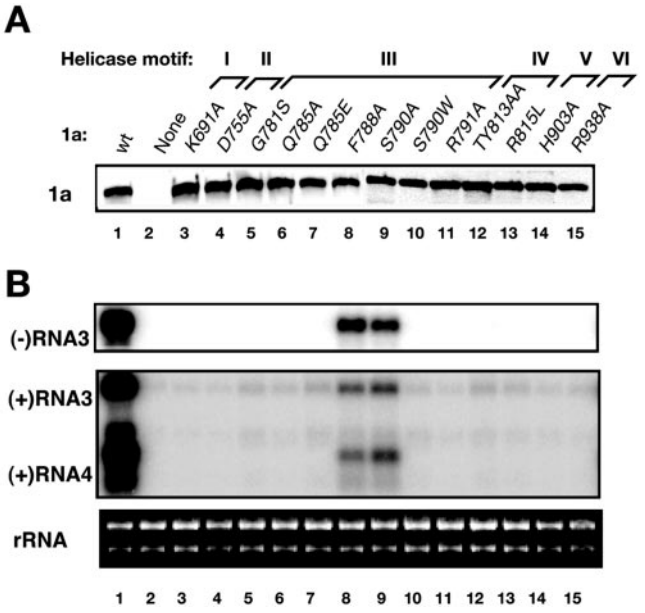

FIG. 2. BMV 1a helicase mutations block RNA replication. (A) Accumulation of wt 1a (lane 1) and 1a helicase mutants (lanes 3 to 15) in yeast cells. Total proteins were extracted from equal numbers of yeast cells expressing either 1a or 1a helicase mutants and analyzed by SDS-PAGE and immunoblot analysis with anti-1a antiserum. (B) Detection of negative- and positive-strand BMV RNA synthesis. Total RNA was extracted from yeast cells expressing $2a^{pol}$, RNA3, and either wt 1a or a 1a helicase mutant. Accumulation of RNA4 and positive- and negative-strand RNA3 were detected by Nothern blotting using probes specific to BMV RNAs. Note that to allow visualization of the RNA bands, the blot showing negative-strand accumulation was exposed much longer than that for positive strands. The equal loading of total RNA was verified by ethidium bromide staining of ribosomal RNAs. Lanes in panel B correspond to the same samples as in panel A.

In cells expressing BMV 1a and $2a^{pol}$ proteins, RNA3 is used as a template to make negative-strand RNA3, which is then used to make progeny-positive RNA3 and subgenomic RNA4 (24). To test if the mutations shown in Fig. 1B in the 1a NTPase/hel domain affected BMV RNA replication, we used Northern blotting to measure the accumulation of negative- and positive-strand BMV RNAs in yeast cells expressing $2a^{pol}$, RNA3, and each of the 1a helicase mutants (Fig. 2B). For cells expressing $2a^{pol}$, RNA3, and wt 1a, strong signals were detected for negative- and positive-strand RNA3 and subgenomic RNA4 (Fig. 2B, lane 1). Without 1a, only a weak signal for the initial positive-strand RNA3, which was transcribed from a DNA plasmid, was detected (Fig. 2B, lane 2). Two 1a mutants in helicase motif III partially supported RNA replication: for F788A(III) and S790A(III), 20 to 30% of wt negative-strand RNA3 levels and 10 to 12% of wt positive-strand RNA3 and subgenomic RNA4 levels were detected (Table 1; Fig. 2B, lanes 8 to 9).

As shown previously (3), K691A(I), D755A(II), and G781S (III) did not support BMV RNA replication. No negative-strand RNA3 or subgenomic RNA4 was detected in yeast cells

TABLE 1. Effects of 1a NTPase/hel mutations on BMV RNA replication, RNA3 protection, spherule sizes, ATPase activity, and interference with RNA3 stabilization by wt 1a

1a or 1a helicase mutant	NTPase/hel motif altered	Negative-strand accumulation (% of wt)	1a-mediated RNA3 stabilization[a] (% of wt)	RNA3 membrane association (% of total)[b]	RNA3 protection (MNase-treated pellet RNA3/pellet RNA3 × 100)	Avg spherule diam[c] (nm)	ATPase activity (% of wt)	Interference with RNA3 accumulation[d]
wt		100	100	73	85	76 ± 16	100	105
Without 1a		ND[e]	0	1	ND	ND	0	100
K691A	I	ND	3.7	22	20	80 ± 12	18	33
D755A	II	ND	3.9	23	12	80 ± 11	9	27
G781S	III	ND	14.1	44	34	83 ± 13	24	65
Q785A	III	ND	4.4	50	17	84 ± 9	35	31
Q785E	III	ND	7.6	38	14	74 ± 11	22	35
F788A	III	30	63	71	49	78 ± 13	67	86
S790A	III	22	65	75	53	81 ± 11	37	124
S790W	III	ND	4.7	31	19	90 ± 12	26	82
R791A	III	ND	2.6	1	ND	74 ± 12 34 ± 7[f]	110	64
TY813AA	IV	ND	2.8	7	ND	ND	102	35
R815L	IV	ND	1.1	19	ND	ND	158	24
H903A	V	ND	6.0	12	20	79 ± 9	55	82
R938A	VI	ND	4.3	6	ND	ND	52	49

[a] The following equation was used to calculate 1a-mediated RNA3 stabilization: [(RNA3 signal with 1a helicase mutant − RNA3 signal without 1a) ÷ (RNA3 signal with 1a wt RNA3 signal without 1a)] × 100%.

[b] RNA3 membrane association was calculated as follows: [RNA3 signal in pellet ÷ (RNA3 signal in pellet + RNA3 signal in supernatant)] × 100% − [18S rRNA signal in pellet ÷ (18S rRNA signal in pellet + 18S rRNA signal in supernatant)] × 100%.

[c] For wt 1a and each 1a mutant, thin-section electron microscopy was used to measure the diameter of 45 to 65 spherules.

[d] Interference with RNA3 accumulation was measured as follows: [(RNA3 signal in cells expressing wt 1a and an indicated 1a helicase mutant) ÷ (RNA3 signal in cells expressing one copy of wt 1a)] × 100%.

[e] ND, not detected.

[f] As described in Results, R791A made spherules of two distinct size classes.

expressing any of these three 1a mutants (Fig. 2B, lanes 3 to 5). We further found that all of the remaining Fig. 1B mutations in motifs III, IV, V, and VI blocked RNA3 replication as well as the above three mutants, showing that each of these motifs is critical for 1a to function properly in BMV RNA replication (Fig. 2B). In the experiments described in the following sections, we tested other 1a functions to determine which step(s) of replication was blocked by each of these replication-defective mutations.

All 1a helicase mutants were targeted to the ER membrane. In yeast and plant cells, 1a localizes to perinuclear ER membranes, colocalizing with ER markers in membrane flotation and immunofluorescent staining (9, 48, 49).

We first performed membrane flotation assays to determine whether the 1a helicase mutants associated with membrane. Yeast cells expressing wt 1a or the 1a mutants were spheroplasted and lysed, and the total lysate was loaded at the bottom of OptiPrep density gradients. Using conditions under which membranes float to the top of the gradient and soluble proteins sediment to the bottom of the gradient (5), most of wt 1a was detected in the top two fractions paralleling the distribution of an ER marker, Dpm1p (Fig. 3A and B). Similarly, all 1a helicase mutants (Fig. 1B), as illustrated in Fig. 3B for K691A(I), D755A(II), Q785E(III), and F788A(III), were detected mainly in the first two gradient fractions, paralleling the distribution of wt 1a. Thus, all of these 1a mutants remained membrane associated at wt levels.

To further determine whether these 1a helicase mutants were specifically associated with ER membranes, we used confocal immunofluorescence microscopy to determine the location of the 1a mutants. wt 1a was mainly associated with perinuclear ER membrane and, to a lesser degree, peripheral ER membrane, matching the distribution of ER marker Sec63p (Fig. 3C, first row). Like wt 1a, all 1a helicase mutants similarly localized to perinuclear ER membranes, as illustrated in Fig. 3C for three mutants, K691A(I), R815L(IV), and R938A(VI). Thus, membrane flotation and confocal microscopy assays collectively indicated that all of these 1a mutants were functional in terms of ER membrane association.

All 1a helicase mutants recruited $2a^{pol}$ to membrane. wt 1a recruits $2a^{pol}$ to the membrane by interacting via its NTPase/hel domain with the $2a^{pol}$ N terminus (7, 27). Cell fractionation and Western blotting were used to examine the distribution of $2a^{pol}$ without 1a, with wt 1a, or with each 1a helicase mutant (Fig. 4). After centrifugation of cell lysate, $2a^{pol}$ expressed without 1a was exclusively detected in the supernatant fraction, similar to soluble protein Pgk1p and contrary to ER marker Dpm1p, which accumulates mainly in the membrane-enriched pellet fraction (Fig. 4) (7). In the presence of wt 1a, two effects were observed. First, as noticed previously (23), $2a^{pol}$ accumulation increased two- to threefold. Second, $2a^{pol}$ was mainly present in the membrane-enriched pellet, indicating that $2a^{pol}$ was recruited to membrane by 1a (Fig. 4) (7). The recruitment of $2a^{pol}$ by 1a was specific because Pgk1p was still in the supernatant when 1a was present (data not shown) (7). When coexpressed with any of the 1a helicase mutants, as illustrated in Fig. 4 for F788A(III), TY813AA(IV), R815L(IV), and R938A(VI), $2a^{pol}$ accumulation similarly increased two- to threefold, and $2a^{pol}$ was present primarily in the membrane-enriched pellet (Fig. 4), indicating that all of the 1a helicase mutants were functional in $2a^{pol}$ recruitment to membranes.

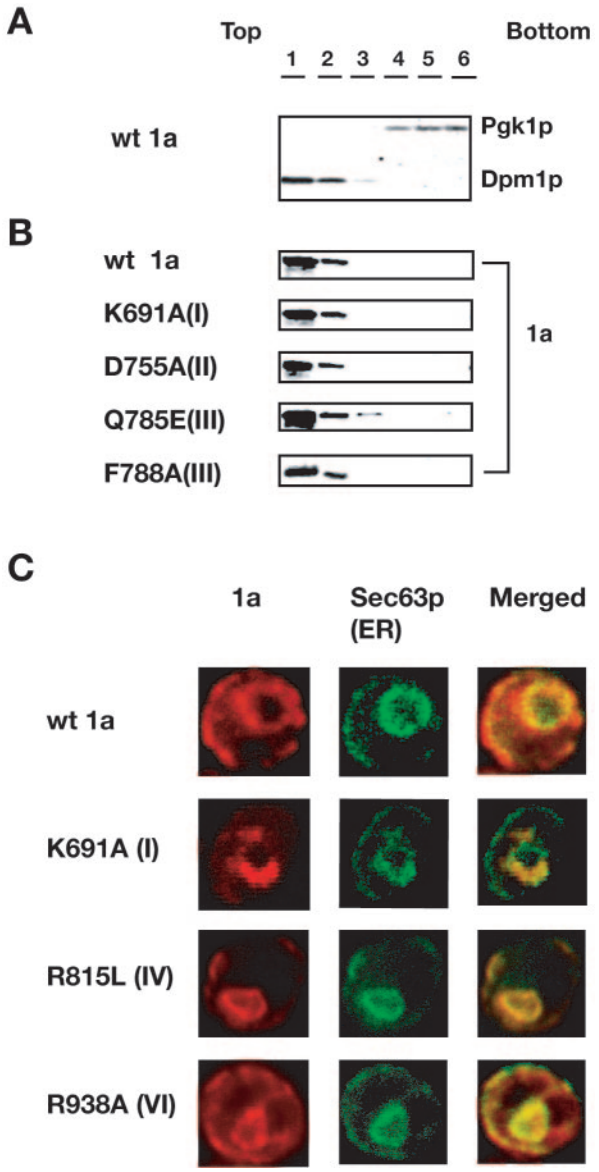

FIG. 3. ER membrane association of 1a helicase mutants. Lysates of yeast cells expressing either 1a wt or the indicated 1a helicase mutants were mixed with 2 volumes of 60% OptiPrep in lysis buffer and overlaid by 4 volumes of 30% OptiPrep in lysis buffer. After being centrifuged for 5 h in a Beckman TLS55 rotor at 55,000 rpm, the gradient was divided into six fractions from top to bottom. Aliquots of each fraction were analyzed by SDS-PAGE and Western blotting, using either antibodies against Dpm1p, an ER membrane protein, and Pgk1p, a soluble protein (A) or antiserum against BMV 1a (B). (C) The localization of 1a in yeast cells coexpressing Sec63p-GFP and either wt 1a or the indicated 1a helicase mutant was examined by indirect immunofluorescence with a confocal microscope with secondary antibody conjugated with Texas red. The distribution of Sec63p-GFP was detected by GFP fluorescence. The merged images were generated by the superimposition of both signals. The yellow color indicates the colocalization of 1a and Sec63p-GFP.

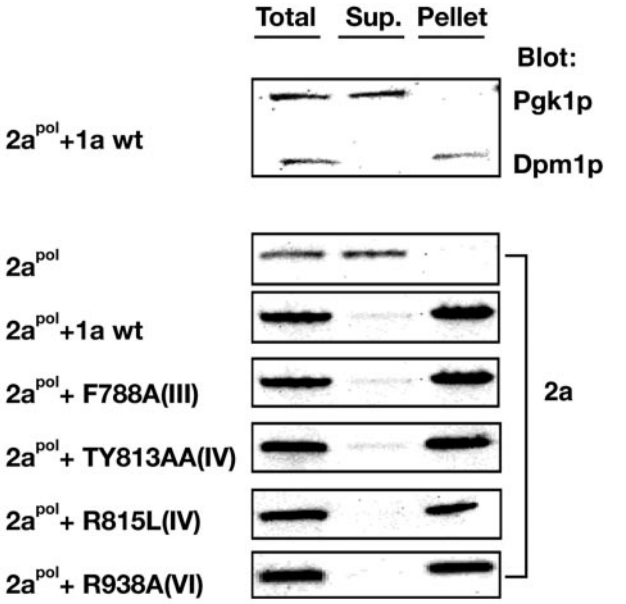

FIG. 4. Recruitment of $2a^{pol}$ to the membrane fraction by 1a helicase mutants. Yeast cells expressing only $2a^{pol}$ or coexpressing $2a^{pol}$ and either wt 1a or the indicated 1a helicase mutants were spheroplasted and lysed osmotically to yield a total protein fraction (Total). The lysate was centrifuged for 5 min at 20,000 $\times$ *g* to obtain a membrane-depleted supernatant (Sup) and membrane-enriched pellet (Pellet). Equal volumes of Total, Sup, and Pellet fractions were subjected to SDS-PAGE and immunoblotted with antibodies against Pgk1p, Dpm1p, and BMV 1a, as indicated on the right.

Effect of helicase mutations on 1a-mediated RNA3 protection. In yeast cells, coexpressing wt 1a increases the RNA3 half-life from 5 to 7 min in the absence of 1a to >3 h, and increases RNA3 accumulation by 8 to 30 fold, depending on the level of 1a expressed (25, 52). As shown in Fig. 5A, lanes 1 to 2, expressing wt 1a from the relatively strong, GAL-induced *GAL1* promoter increased RNA3 accumulation about 20 fold over cells lacking 1a. Similarly, the two 1a mutants that partially supported BMV RNA replication, F788A(III) and S790A(III) (Table 1 and Fig. 5A, lanes 8 to 9), increased RNA3 accumulation by 13 fold (i.e., 63 to 65% of wt 1a) (Table 1). In addition, one replication-defective mutant, G781S(III), increased RNA3 accumulation by threefold (14% of wt 1a) (Table 1 and Fig. 5A, lane 5). However, for the remaining replication-defective mutants, RNA3 accumulation was not significantly increased over the RNA3 level in cells lacking 1a (1 to 8% of RNA3 levels with wt 1a) (Table 1 and Fig. 5A).

The 1a-stimulated increase in RNA3 accumulation in vivo is associated with 1a-induced transfer of RNA3 to a membrane-associated, nuclease-resistant state (52). This membrane-associated, nuclease-resistant state is indistinguishable from that of nascent BMV RNA3 molecules, which are localized inside the ER membrane-bounded, spherular RNA replication complexes (52). To test the fate of RNA3 in yeast cells expressing 1a helicase mutants, we centrifuged total yeast lysates to yield a membrane-depleted soluble supernatant and a membrane-enriched pellet. In yeast cells lacking 1a, RNA3 was exclusively in the supernatant and was readily degraded by the addition of MNase (Fig. 5B and C). In contrast, in yeast cells expressing wt 1a, ~73% of RNA3 was recovered in the pellet; of this membrane-associated RNA3, ~85% was protected from MNase degradation. Only a small fraction of RNA3 was recovered in the supernatant, and most of this was digested by the added

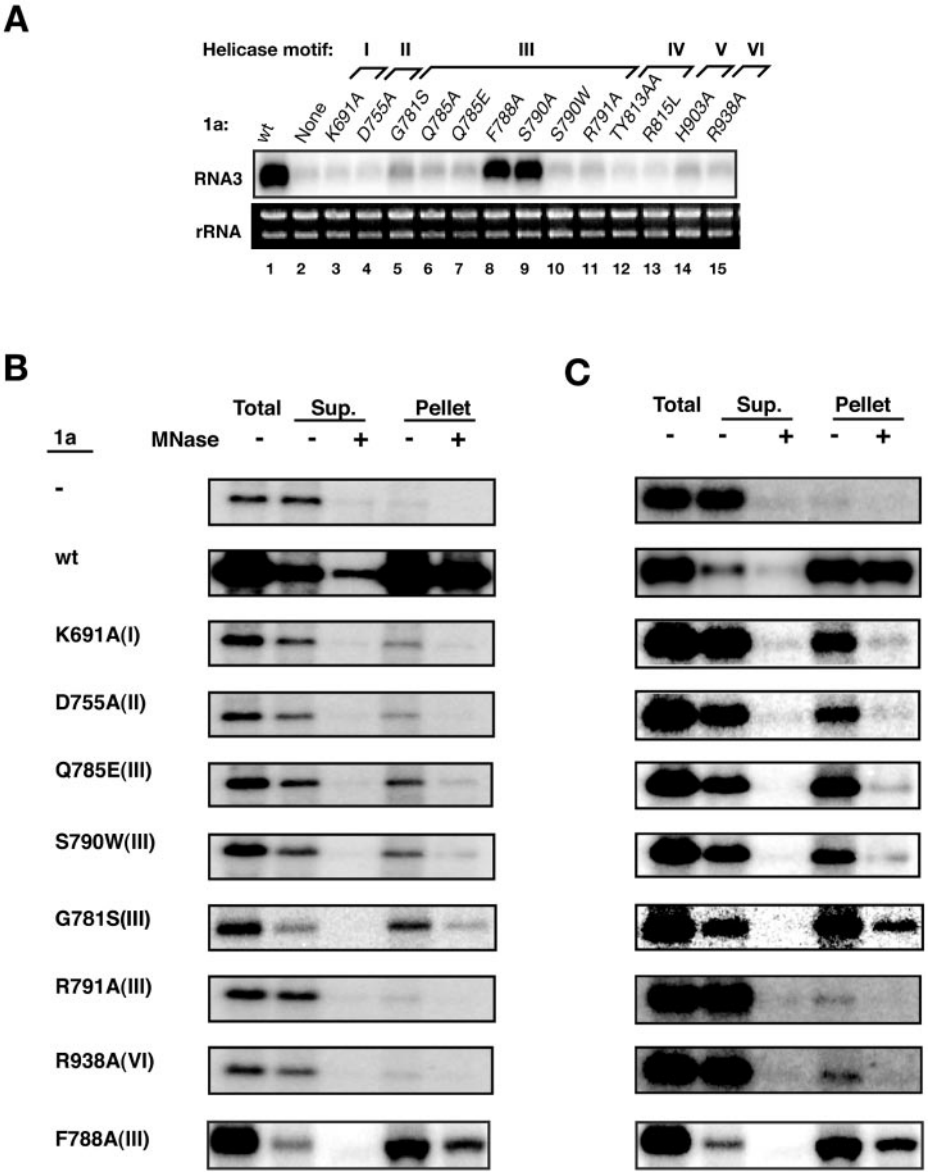

FIG. 5. Yeast cells expressing replication-defective 1a helicase mutants failed to recruit viral RNA to the membrane-associated, RNase-resistant state. (A) Total RNA was isolated from yeast cells expressing RNA3 and 1a or the indicated 1a helicase mutant. Equal amounts (each, 2 μg) of total RNA were used for Northern blot detection of RNA3, and equal loading of the total RNA was verified by ethidium bromide staining of ribosomal RNAs. Note that the level of 1a-stabilized RNA3 in the absence of $2a^{pol}$ is ~10- to 12-fold lower than the level of RNA produced by full replication (Fig. 2B) (25, 52). (B) Yeast cells coexpressing RNA3 and wt 1a or the indicated 1a helicase mutant were spheroplasted and osmotically lysed. Total lysate was divided into supernatant (Sup) and membrane-enriched pellet (Pellet) by a 20,000 × *g* centrifugation and treated with MNase at 30°C. The RNA3 level in each fraction was analyzed by Northern blotting. (C) The same Northern blots as in panel B are shown, but with signal intensities increased to facilitate assessment of nuclease resistance or susceptibility in the pellet fractions (right two lanes). To facilitate comparisons between wt 1a and 1a mutants, signal intensities were adjusted to provide similar intensities of RNA3 signals in the lanes not tested with nuclease.

MNase (Fig. 5B and C). In yeast cells expressing F788A(III), and S790A(III), which partially support RNA replication (Fig. 2B) and stabilize RNA3 nearly as well as that of wt 1a (Fig. 5A), RNA3 similarly was efficiently recovered in the membrane pellet in a highly nuclease-resistant state (Fig. 5B and C; Table 1).

By contrast, the replication-defective mutants could be divided into two groups. The first group included R791A(III), TY813AA(IV), and R938A(VI). In yeast cells with these 1a mutants, RNA3 was mainly detected in the supernatant, and only about 1 to 7% of RNA3 was present in the membrane-enriched pellet, similar to RNA3 without 1a (Table 1; Fig. 5B to C), while about 73% of RNA3 was recovered from the pellet in yeast cells expressing wt 1a. Thus, these mutations largely blocked 1a-mediated targeting of RNA3 to membranes.

The second group included K691A(I), D755A(II), G781S(III), Q785A(III), Q785E(III), S790W(III), R815L(IV), and H903A (V), for which a greater fraction of RNA3 was recovered in

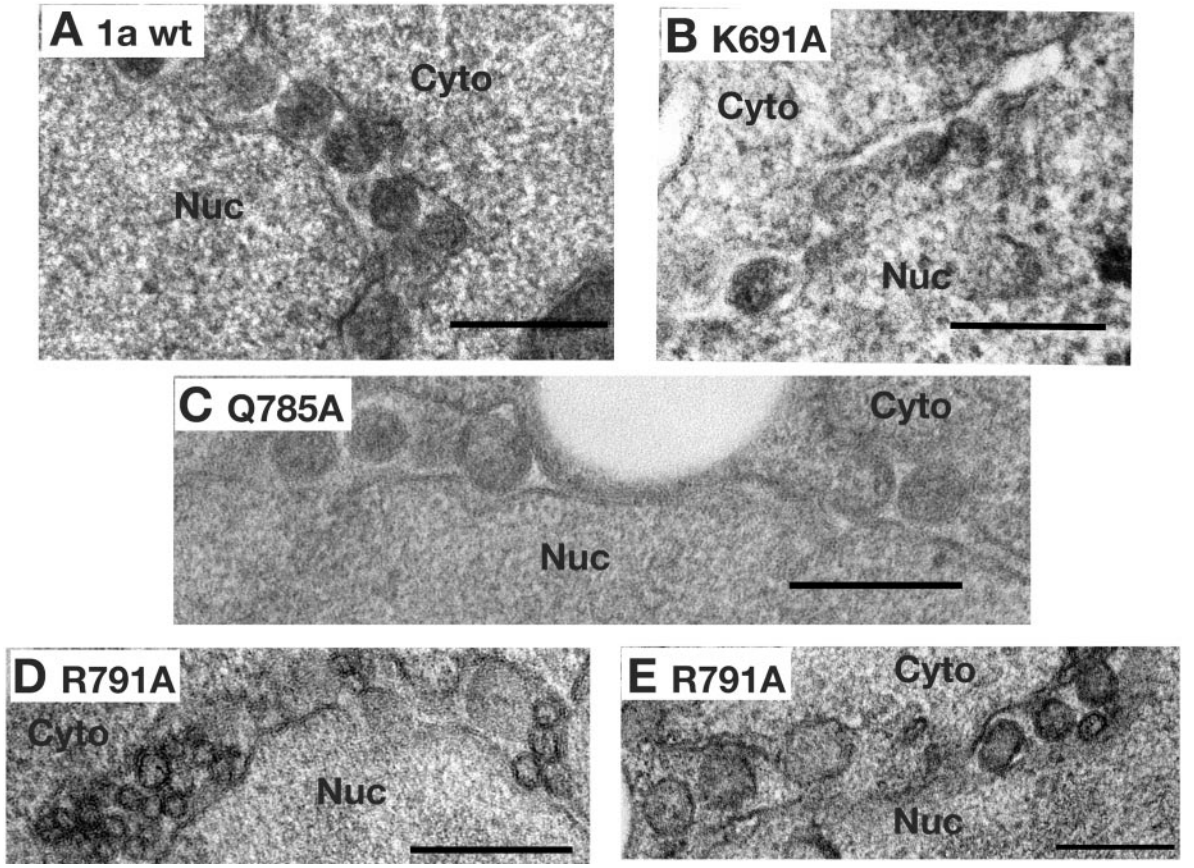

FIG. 6. Spherule formation in yeast cells expressing 1a helicase mutants. Yeast cells expressing wt 1a or the indicated 1a helicase mutant were examined by EM following osmium staining. Labels indicate nucleoplasm (Nuc) and cytoplasm (Cyto). Bars, 200 nm. wt 1a (A), K691A(I) (B), Q785A(III) (C), and R791A(III) (D and E) are shown.

the pellet fraction, ranging from 12% to 50% of total RNA3. The presence of as high as 0.15 M or 0.45 M salt did not change the amount of membrane-associated RNA3 (data not shown). In yeast cells with mutant G781S(III), which increased RNA3 accumulation threefold, more RNA3 was targeted to membrane (44% of total RNA3) and protected (35% of membrane-associated RNA3) than with other mutants (Table 1). Nevertheless, for all other 1a mutants in this second group, the membrane-associated RNA3 was almost completely degraded by added MNase (Table 1 and Fig. 5B and C). Thus, these 1a mutants showed various levels of defects in recruiting RNA3 to membranes but all were substantially defective in protecting RNA3 from added nuclease, implying that these two steps are functionally separable.

Spherule formation in yeast cells expressing 1a helicase mutants. As noted in the introduction, 1a is necessary and sufficient to induce the formation of the 50- to 70-nm ER membrane invaginations (spherules) that serve as BMV RNA replication compartments (52). To test whether the replication-defective mutants lost the ability to induce viral spherule formation, we examined yeast cells expressing each of these 1a mutants by EM (Fig. 6) and determined the diameter of 45 to 60 spherules for each mutant (Table 1). Most 1a helicase mutants induced the formation of spherules of wt size and frequency, as illustrated in Fig. 6B and C for K691A(I) and Q785A(III). Similarly, spherules of normal frequency and size (i.e., within ±10% of average wt diameter) were observed for D755A(II), G781S(I), Q785E(III), Q785A(III), F788A(III), S790A(III), and R903(V). S790W(III) induced formation of spherules whose diameter was 120% of that induced by wt 1a (Table 1). More notably, mutant R791A(III) made spherules of two distinct sizes. The larger ones (Fig. 6E) were similar in size to those induced by wt 1a, while the smaller ones (Fig. 6D) were about one-half to one-third of wt size. Most cells examined contained both sizes of spherules, usually with the smaller spherules in excess (Fig. 6D and Table 1). The reason for forming two types of spherules is currently unclear. In yeast cells expressing any of three 1a mutants, TY813AA(IV), R815L(IV), and R938A(VI), no spherules were observed after extensive effort, showing that these mutants either do not induce spherule formation or do so at a frequency that is too low to detect. Interestingly, confocal microscopy showed that all three mutants were still colocalized with the ER marker Sec63p and recruited $2a^{pol}$ protein to the membrane fraction (Fig. 3C and 4).

Effect of 1a helicase mutations on ATPase activity. All known helicases possess NTPase activity, which is necessary for their function. The 1a NTPase/hel domain also contains consensus Walker A and B motifs (motifs I and II, respectively) of NTPase (17, 31). However, 1a NTPase activity has not been demonstrated.

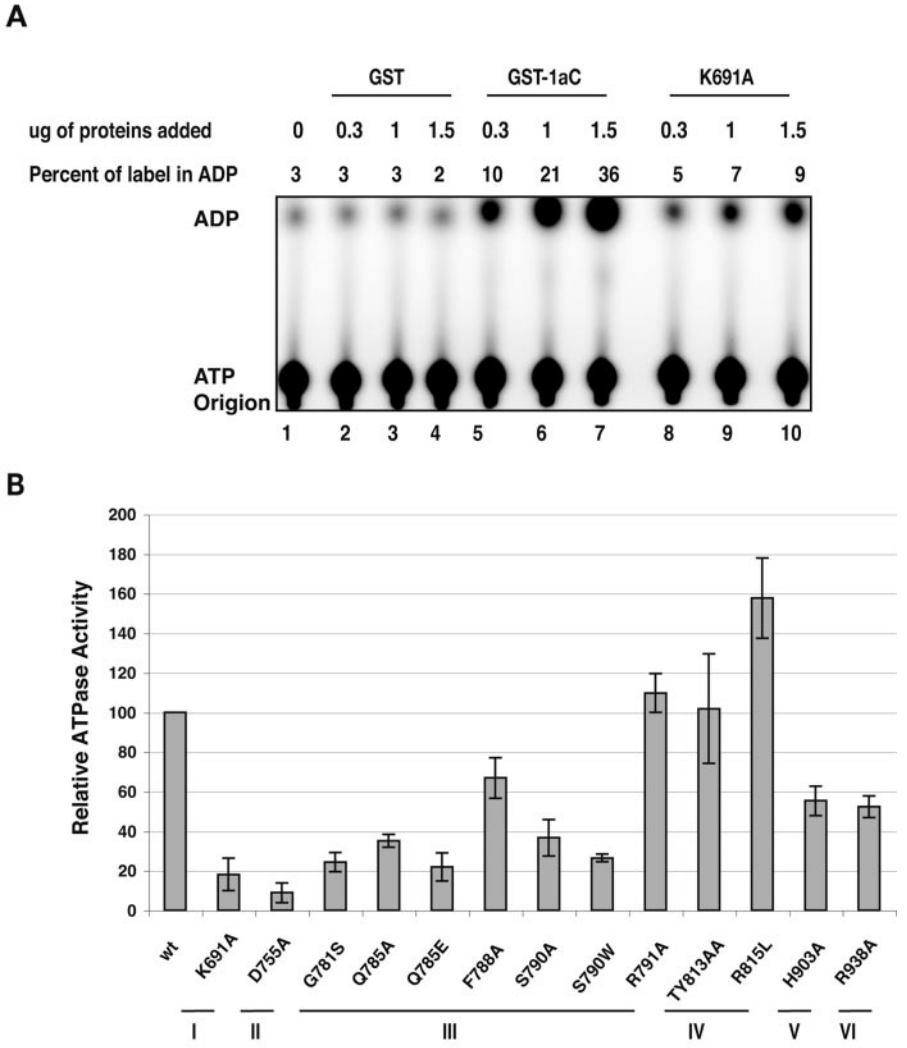

FIG. 7. ATPase activities of wt 1a and 1a helicase mutants. (A) ATPase assay. No protein (lane 1) or the indicated amounts of GST (lanes 2 to 4), GST-1aC (lanes 5 to 7), or GST-1a-K691A (K691A) were incubated with [α-^{32}P]ATP at 37°C for 30 min. Aliquots of the reaction mixtures were analyzed by TLC, and the percentage of ADP released was used to measure ATPase activity. (B) ATPase activity of each 1a helicase mutant. ATPase activity was assayed three times for each mutant; error bars represent standard deviations. All data were normalized by subtracting the background percentage of ADP present in the absence of added protein or in the presence of GST alone (A) from the percentage of ADP released by 1a wt and helicase mutants.

To test the BMV 1a helicase domain for NTPase activity, we developed an ATPase assay using *E. coli*-expressed, purified, GST-tagged, C-terminal 1a fragment GST-1aC, which contains the C-terminal 424 to 961 amino acids of 1a, including the NTPase/hel domain. The percentage of ATP hydrolyzed to ADP was used to measure ATPase activity. In a mock reaction mixture without any protein, about 3% of the radioactive label was found in ADP, which was probably an autohydrolysis product. GST-1aC demonstrated a dose-dependent ATPase activity, with 0.3 to 1.5 μg of protein releasing 10 to 36% of the label as ADP (Fig. 7A, lanes 5 to 7). Increasing amounts of nonfused GST protein yielded only 2 to 3% of label compared to ADP (Fig. 7A, lanes 8 to 10), similar to a mock reaction, indicating that ATPase activity is specific to that of the purified BMV 1a fragment. After we corrected for this nonspecific background, a motif I mutant fragment, GST-1aC-K691A (K691A), inhibited ATPase activity by >80% (Fig. 7A, lanes 8 to 10). Thus, the purified BMV 1a fragment 1aC has ATPase activity. In the same assay, the activity of GST-1aC with CTP or GTP was similar to that with ATP, while the activity with UTP was ~70% of that for ATP.

The effect of the 1a mutations in this NTPase activity generally followed the expectations from mutagenesis of the corresponding motifs in other helicases (6, 11, 12, 20, 37, 41, 50, 55). K691A(I) and D755A(II) lost most of their ATPase activity, retaining only 20% and 10% of wt activity (Fig. 7B) (20, 37, 41, 50, 55). By contrast, mutations in motif IV (TY813AA and R815L) did not inhibit ATPase activity at all, while mutations in motifs V and VI (H903A and R938A) only inhibited ATPase activity twofold (Fig. 7B) (6). Mutations in motif III had various effects. The ATPase activity of R791A was similar to that of wt 1a, while G781S, Q785A, Q785E, and S790W

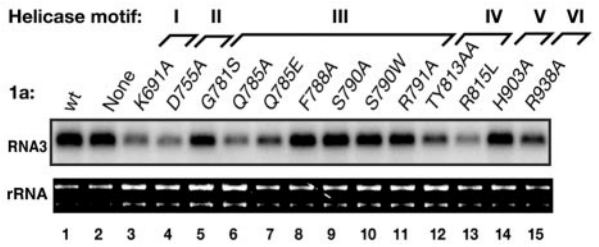

FIG. 8. 1a helicase mutants inhibit in *trans* the ability of wt 1a to stabilize RNA3. Total RNA was isolated from yeast cells expressing RNA3, wt 1a, and a 1a helicase mutant as indicated. Northern blotting was used to examine the accumulation of RNA3 with a BMV RNA-specific probe. The equal loading of total RNA was verified by ethidium bromide staining of ribosomal RNAs.

showed 20 to 35% of wt 1a activity (Fig. 7B) (11, 12). Two mutants, F788A and S790A, which partially supported RNA replication and 1a-mediated RNA3 protection, retained 40 to 70% of wt activity (Fig. 7B).

***trans* interference by 1a helicase mutants with 1a-stimulated RNA3 accumulation.** Previously, K691A(I) was found to interfere with BMV RNA replication, with only about 20% of RNA3 replication remaining in yeast cells expressing both wt 1a and K691A(I) (3). Here, we tested if K691A(I) and the other Fig. 1B mutants interfered with BMV RNA template recruitment and protection, which are reflected by 1a stimulation of viral RNA template accumulation. In yeast cells expressing two wt 1a alleles, RNA3 accumulation increased only slightly, compared to that of one copy of wt 1a (Table 1 and Fig. 8, lanes 1 to 2). This is consistent with the prior finding that negative-strand RNA synthesis increased by only about 20% in cells expressing 1a from two plasmids (3). Coexpression of 1a mutants retaining significant RNA3 stabilization activity [F788A(III) and S790A(III)] (Fig. 5A) yielded RNA3 accumulation similar to that of wt 1a alone (90 to 120% of wt 1a) (Table 1 and Fig. 8). A second group of mutants, including G781S(III), S790W(III), R791A(III), H903A(V), and R938A (VI), showed modest interference with the ability of wt 1a to stimulate RNA3 accumulation. On coexpression of these 1a mutants with wt 1a, RNA3 accumulation was 50 to 80% of that in cells expressing wt 1a alone. A third group of 1a mutants, including K691A(I), D755A(II), Q785A(III), Q785E(III), TY813AA(IV), and R815L(IV), displayed a more severe dominant negative effect on the ability of wt 1a to stimulate accumulation, reducing RNA3 accumulation to only 20 to 35% of that in cells expressing wt 1a alone (Table 1; Fig. 8, lanes 3 to 4, 6 to 7, and 12 to 13). The potential implications of such trans interference are considered below (see Discussion).

DISCUSSION

Virus-encoded NTPase/hel domains are essential for RNA replication by many positive-strand RNA viruses. For the NS3 helicases of flaviviruses (19, 20, 41), for example, mutations that abolish NTPase or NTPase and helicase activities also block viral RNA replication.

Mutations in the BMV 1a NTPase/hel domain block RNA replication by interfering with both replication complex assembly (3) and the function of preassembled replication complexes (34). In this study, we used mutational analysis to examine the roles of the BMV 1a NTPase/hel domain in early steps of RNA replication complex assembly. The results show that mutating conserved residues in each of six tested helicase motifs did not inhibit 1a localization to ER membranes or $2a^{pol}$ recruitment and in most cases did not inhibit 1a-induced ER membrane invagination to form the spherule compartments in which BMV RNA replication occurs. Mutations in motifs IV (TY813AA and R815L), V (H903A), and VI (R938A) did not affect ATPase activity. However, each of these helicase motifs was crucial for 1a to recruit viral RNA templates to a membrane-associated, RNase-resistant state. As discussed below, the data further suggest that 1a recruitment of viral RNA may involve at least two mechanistically separable steps that are dependent on the 1a NTPase/hel domain, such as RNA binding and subsequent translocation into a preformed replication compartment.

1a NTPase/hel mutations and spherule formation. 1a is the only viral factor required to induce ER membrane invaginations to form viral spherules and is present at a level of hundreds of copies per spherule (52). However, the mechanism of spherule formation is not understood. Most of the replication-defective 1a NTPase/hel mutants made wt spherules, including K691A(I), D755A(II), and Q785E(III). In the crystal structures of related helicases, the amino acid corresponding to 1a K691 interacts with the ATP phosphates, while the correlate of D755 coordinates Mg^{2+} and that of Q785 contacts the ATP γ-phosphate (6, 32, 58). Mutations at the equivalent amino acids block NTPase activities in multiple helicases (11, 20, 37, 41, 50, 55). Similarly, we found that the ATPase activity of mutants K691A(I), D755A (II), and Q785E(III) was only 10 to 25% of that of wt 1a (Fig. 7B). Thus, the unimpaired spherule formation by the corresponding 1a mutants implies that NTPase activity is not required for spherule formation and that the energy to perform the associated membrane rearrangements must be derived from other interactions.

Three 1a mutants, TY813AA(IV), R815L(IV), and R938A (VI), did not induce detectable spherule formation even though they still associated with perinuclear ER membranes (Fig. 3C) and possessed wt or near-wt ATPase activity (Fig. 7B). It is possible that motifs IV and VI are involved selectively in spherule formation. Alternatively, these mutations may affect relevant 1a functions unrelated to helicase activity, such as 1a-1a interactions (46).

Mutant S790W(III) made spherules significantly larger than those of the wild type (with 95% confidence) (Table 1). Moreover, another mutation in motif III, R791A(III), made some normal spherules plus an excess of smaller spherules that were only 33 to 50% of the wt diameter. Thus, motif III appears to have a function affecting spherule size. Multiple results imply that motif III bridges ATPase activity to double-stranded nucleic acid displacement (6, 11, 58). The alteration of spherule size by motif III mutants suggests that this function has unexpected links to spherule size, or that 1a motif III has additional functions, or that these motif III mutations alter 1a folding, 1a-1a interactions, or 1a-host interactions.

1a NTPase/hel mutations block RNA recruitment to a membrane-associated, nuclease-resistant state. All tested 1a mutations in motifs I, II, IV, V, and VI and most mutations in motif III blocked detectable RNA replication (Fig. 2B). Moreover, although all of these replication-defective 1a mutants localized

to perinuclear ER membranes (Fig. 3B and C) and their NTPase/hel domains recruited $2a^{pol}$ (Fig. 4) with wt efficiency, all were seriously defective in recruiting and stabilizing RNA3, yielding only 1 to 14% of the increase in RNA3 accumulation induced by wt 1a (Table 1 and Fig. 5A).

The phenotypes of these 1a NTPase/hel mutations suggest that 1a-mediated RNA recruitment and stabilization may involve at least two distinguishable steps. For example, despite their membrane association, 1a mutants R791A(III), TY813AA(III), and R938A(VI) failed to induce RNA3 to fractionate with membranes at levels significantly above those found in the absence of 1a (Table 1; Fig. 5B and C). These 1a mutants may have lost either the ability to recognize viral RNA templates via the RE element or general RNA binding activities. Altered RNA binding is particularly possible for 1a mutant R791A, since the corresponding amino acid in the PcrA (R260) and Rep helicase (R251) crystal structures contacts ssDNA (32, 58).

A second group of mutants, K691A(I), D755(A), G781S (III), Q785A(III), Q785E(III), S790W(III), R815L(IV), and H903A(V), recruited reduced but detectable levels of RNA3 to membranes (Table 1 and Fig. 5B). However, in striking contrast to wt 1a, most if not all of the membrane-associated RNA3 recruited by these 1a mutants was degraded by added nuclease. Thus, these 1a mutants separated 1a-induced RNA recruitment to membranes from 1a-induced RNA protection, revealing a membrane-associated but nuclease-susceptible RNA3 pool not detected with wt 1a. At least two possibilities could explain this observation. First, these mutations may interfere with a step between 1a recruitment of RNA3 to an initial, membrane-associated, but nuclease-susceptible state and subsequent RNA3 transfer to a more nuclease-resistant state such as the spherule interior. Alternatively, there may be only one state or compartment for membrane-associated RNA3, and these mutants make this compartment more accessible to nuclease.

Possible parallels with RNA recruitment by dsRNA phage ϕ6 NTPase/hel P4. An expanding list of putative helicases may not be involved in duplex unwinding, but rather in RNA or DNA translocation, modulating RNA-protein interactions, or other functions (13, 14, 16, 39, 53, 56). Moreover, a wide variety of ds- and ssDNA viruses and dsRNA viruses use hexameric NTPases or NTPase complexes to package their nucleic acid into preformed empty capsids (26, 29, 43). In at least some of these cases, the NTPase activity is related to helicase functions. For example, ssDNA packaging into adenovirus-associated virus 2 requires the DNA helicase activity of the viral Rep52/40 complex (29).

For dsRNA cystoviruses like ϕ6, positive-strand precursors of the viral genomic RNAs are packaged into preformed empty capsids in a reaction requiring a hexameric viral NTPase, P4, located at the 12 icosahedral vertices of the capsid. Purified P4 hexamers translocate along RNA in a 5′-to-3′ direction and can act as helicases, displacing base-paired strands (26). This directionality is potentially consistent with the location of virus-specific packaging signals at the 5′ ends of ϕ6 positive-strand genome precursors. After packaging, negative strands are synthesized, and the resulting dsRNA is used to transcribe more positive RNA. P4 is essential not only for RNA packaging but also for positive-strand synthesis, likely because it facilitates positive-strand export, just as the portal NTPase complexes of DNA viruses govern both DNA packaging and DNA exit from the capsid (47).

The 1a NTPase/hel domain shows intriguing parallels with ϕ6 P4 NTPase/hel. Like P4 (47), an active 1a NTPase/hel domain is required both for recruiting the initial positive-strand viral RNA templates into an RNA synthesis compartment (Fig. 5B and C) (3) and for subsequent positive-strand RNA synthesis (34). The corresponding NTPase/hel domain of tobacco mosaic virus p126, a 1a homolog (1), forms hexamers with RNA helicase activity (18). Consistent with this, the *trans* interference of 1a-mediated RNA3 stabilization by some 1a helicase mutants suggests that 1a may act on RNA3 as a multimer (Fig. 8). Our findings here that mutations in the 1a helicase motifs allow spherule formation and 1a recruitment of RNA to membranes but prevent 1a from transferring RNA3 to a nuclease-resistant state are consistent with the possibility that, like P4, the 1a NTPase/hel domain translocates viral RNAs into a preformed replication compartment. Also consistent with the possibility that the spherule replication compartments may be formed prior to BMV RNA recruitment is the fact that 1a forms spherules in vivo with equal efficiency in the presence or absence of BMV RNAs (52). Like the packaging signals on ϕ6 positive-strand RNAs, the 1a-responsive RE elements that direct recruitment of BMV RNA1 and RNA2 for replication are located at the extreme 5′ ends (8). For BMV RNA3, the 1a-responsive RE element is located internally but appears to communicate with the 5′ end (10, 54).

ACKNOWLEDGMENTS

We thank Billy Dye for comments on the manuscript, Benjamin Kopek for making mutants TY813AA and R815L, Michael Triebwasser for general assistance, and all members of our laboratory for discussions and suggestions. We also thank Randall Massey and Benjamin August of the University of Wisconsin Medical School Electron Microscope Facility for assistance with EM work, Lance Rodenkirch of the W. M. Keck Laboratory for Biological Imaging for assistance with confocal microscopy, and Pamela Silver of Harvard Medical School for providing the Sec63p-GFP plasmid.

This work was supported by NIH grant GM35072. P.A. is an Investigator of the Howard Hughes Medical Institute.

REFERENCES

1. **Ahlquist, P., E. G. Strauss, C. M. Rice, J. H. Strauss, J. Haseloff, and D. Zimmern.** 1985. Sindbis virus proteins nsP1 and nsP2 contain homology to nonstructural proteins from several RNA plant viruses. J. Virol. **53:** 536–542.
2. **Ahola, T., and P. Ahlquist.** 1999. Putative RNA capping activities encoded by brome mosaic virus: methylation and covalent binding of guanylate by replicase protein 1a. J. Virol. **73:**10061–10069.
3. **Ahola, T., J. A. den Boon, and P. Ahlquist.** 2000. Helicase and capping enzyme active site mutations in brome mosaic virus protein 1a cause defects in template recruitment, negative-strand RNA synthesis, and viral RNA capping. J. Virol. **74:**8803–8811.
4. **Allison, R., C. Thompson, and P. Ahlquist.** 1990. Regeneration of a functional RNA virus genome by recombination between deletion mutants and requirement for cowpea chlorotic mottle virus 3a and coat genes for systemic infection. Proc. Natl. Acad. Sci. USA **87:**1820–1824.
5. **Bagnat, M., S. Keranen, A. Shevchenko, and K. Simons.** 2000. Lipid rafts function in biosynthetic delivery of proteins to the cell surface in yeast. Proc. Natl. Acad. Sci. USA **97:**3254–3259.
6. **Caruthers, J. M., and D. B. McKay.** 2002. Helicase structure and mechanism. Curr. Opin. Struct. Biol. **12:**123–133.
7. **Chen, J., and P. Ahlquist.** 2000. Brome mosaic virus polymerase-like protein 2a is directed to the endoplasmic reticulum by helicase-like viral protein 1a. J. Virol. **74:**4310–4318.
8. **Chen, J., A. Noueiry, and P. Ahlquist.** 2001. Brome mosaic virus protein 1a recruits viral RNA2 to RNA replication through a 5′ proximal RNA2 signal. J. Virol. **75:**3207–3219.

9. **den Boon, J. A., J. Chen, and P. Ahlquist.** 2001. Identification of sequences in Brome mosaic virus replicase protein 1a that mediate association with endoplasmic reticulum membranes. J. Virol. **75:**12370–12381.
10. **Diez, J., M. Ishikawa, M. Kaido, and P. Ahlquist.** 2000. Identification and characterization of a host protein required for efficient template selection in viral RNA replication. Proc. Natl. Acad. Sci. USA **97:**3913–3918.
11. **Dillingham, M. S., P. Soultanas, and D. B. Wigley.** 1999. Site-directed mutagenesis of motif III in PcrA helicase reveals a role in coupling ATP hydrolysis to strand separation. Nucleic Acids Res. **27:**3310–3317.
12. **Dillingham, M. S., P. Soultanas, P. Wiley, M. R. Webb, and D. B. Wigley.** 2001. Defining the roles of individual residues in the single-stranded DNA binding site of PcrA helicase. Proc. Natl. Acad. Sci. USA **98:**8381–8387.
13. **Egelman, E. H.** 2001. Structural biology. Pumping DNA. Nature **409:** 573–575.
14. **Fairman, M. E., P. A. Maroney, W. Wang, H. A. Bowers, P. Gollnick, T. W. Nilsen, and E. Jankowsky.** 2004. Protein displacement by DExH/D "RNA helicases" without duplex unwinding. Science **304:**730–734.
15. **Froshauer, S., J. Kartenbeck, and A. Helenius.** 1988. Alphavirus RNA replicase is located on the cytoplasmic surface of endosomes and lysosomes. J. Cell Biol. **107:**2075–2086.
16. **Gomis-Ruth, F. X., G. Moncalian, R. Perez-Luque, A. Gonzalez, E. Cabezon, F. de la Cruz, and M. Coll.** 2001. The bacterial conjugation protein TrwB resembles ring helicases and F1-ATPase. Nature **409:**637–641.
17. **Gorbalenya, A. E., and E. V. Koonin.** 1993. Helicases: amino acid sequence comparisons and structure-function relationships. Curr. Opin. Struct. Biol. **3:**419–429.
18. **Goregaoker, S. P., and J. N. Culver.** 2003. Oligomerization and activity of the helicase domain of the tobacco mosaic virus 126- and 183-kilodalton replicase proteins. J. Virol. **77:**3549–3556.
19. **Grassmann, C. W., O. Isken, and S. E. Behrens.** 1999. Assignment of the multifunctional NS3 protein of bovine viral diarrhea virus during RNA replication: an in vivo and in vitro study. J. Virol. **73:**9196–9205.
20. **Gu, B., C. Liu, J. Lin-Goerke, D. R. Maley, L. L. Gutshall, C. A. Feltenberger, and A. M. Del Vecchio.** 2000. The RNA helicase and nucleotide triphosphatase activities of the bovine viral diarrhea virus NS3 protein are essential for viral replication. J. Virol. **74:**1794–1800.
21. **Hatta, T., S. Bullivant, and R. E. Matthews.** 1973. Fine structure of vesicles induced in chloroplasts of Chinese cabbage leaves by infection with turnip yellow mosaic virus. J. Gen. Virol. **20:**37–50.
22. **Ho, S. N., H. D. Hunt, R. M. Horton, J. K. Pullen, and L. R. Pease.** 1989. Site-directed mutagenesis by overlap extension using the polymerase chain reaction. Gene **77:**51–59.
23. **Ishikawa, M., M. Janda, M. A. Krol, and P. Ahlquist.** 1997. In vivo DNA expression of functional brome mosaic virus RNA replicons in *Saccharomyces cerevisiae*. J. Virol. **71:**7781–7790.
24. **Janda, M., and P. Ahlquist.** 1993. RNA-dependent replication, transcription, and persistence of brome mosaic virus RNA replicons in S. cerevisiae. Cell **72:**961–970.
25. **Janda, M., and P. Ahlquist.** 1998. Brome mosaic virus RNA replication protein 1a dramatically increases in vivo stability but not translation of viral genomic RNA3. Proc. Natl. Acad. Sci. USA **95:**2227–2232.
26. **Kainov, D. E., M. Pirttimaa, R. Tuma, S. J. Butcher, G. J. Thomas, Jr., D. H. Bamford, and E. V. Makeyev.** 2003. RNA packaging device of double-stranded RNA bacteriophages, possibly as simple as hexamer of P4 protein. J. Biol. Chem. **278:**48084–48091.
27. **Kao, C. C., and P. Ahlquist.** 1992. Identification of the domains required for direct interaction of the helicase-like and polymerase-like RNA replication proteins of brome mosaic virus. J. Virol. **66:**7293–7302.
28. **Kim, K. S.** 1977. An ultrastructural study of inclusions and disease in plant cells infected by cowpea chlorotic mottle virus. J. Gen. Virol. **35:**535–543.
29. **King, J. A., R. Dubielzig, D. Grimm, and J. A. Kleinschmidt.** 2001. DNA helicase-mediated packaging of adeno-associated virus type 2 genomes into preformed capsids. EMBO J. **20:**3282–3291.
30. **Kong, F., K. Sivakumaran, and C. Kao.** 1999. The N-terminal half of the brome mosaic virus 1a protein has RNA capping-associated activities: specificity for GTP and S-adenosylmethionine. Virology **259:**200–210.
31. **Koonin, E. V., and V. V. Dolja.** 1993. Evolution and taxonomy of positive-strand RNA viruses: implications of comparative analysis of amino acid sequences. Crit. Rev. Biochem. Mol. Biol. **28:**375–430.
32. **Korolev, S., J. Hsieh, G. H. Gauss, T. M. Lohman, and G. Waksman.** 1997. Major domain swiveling revealed by the crystal structures of complexes of E. coli Rep helicase bound to single-stranded DNA and ADP. Cell **90:**635–647.
33. **Krol, M. A., N. H. Olson, J. Tate, J. E. Johnson, T. S. Baker, and P. Ahlquist.** 1999. RNA-controlled polymorphism in the in vivo assembly of 180-subunit and 120-subunit virions from a single capsid protein. Proc. Natl. Acad. Sci. USA **96:**13650–13655.
34. **Kroner, P. A., B. M. Young, and P. Ahlquist.** 1990. Analysis of the role of brome mosaic virus 1a protein domains in RNA replication, using linker insertion mutagenesis. J. Virol. **64:**6110–6120.
35. **Kujala, P., T. Ahola, N. Ehsani, P. Auvinen, H. Vihinen, and L. Kaariainen.** 1999. Intracellular distribution of rubella virus nonstructural protein P150. J. Virol. **73:**7805–7811.
36. **Lee, W. M., and P. Ahlquist.** 2003. Membrane synthesis, specific lipid requirements, and localized lipid composition changes associated with a positive-strand RNA virus RNA replication protein. J. Virol. **77:**12819–12828.
37. **Li, Y. I., T. W. Shih, Y. H. Hsu, Y. T. Han, Y. L. Huang, and M. Meng.** 2001. The helicase-like domain of plant potexvirus replicase participates in formation of RNA 5′ cap structure by exhibiting RNA 5′-triphosphatase activity. J. Virol. **75:**12114–12120.
38. **Lin, C., and J. L. Kim.** 1999. Structure-based mutagenesis study of hepatitis C virus NS3 helicase. J. Virol. **73:**8798–8807.
39. **Linder, P.** 2004. Molecular biology. The life of RNA with proteins. Science **304:**694–695.
40. **Marchler-Bauer, A., J. B. Anderson, C. DeWeese-Scott, N. D. Fedorova, L. Y. Geer, S. He, D. I. Hurwitz, J. D. Jackson, A. R. Jacobs, C. J. Lanczycki, C. A. Liebert, C. Liu, T. Madej, G. H. Marchler, R. Mazumder, A. N. Nikolskaya, A. R. Panchenko, B. S. Rao, B. A. Shoemaker, V. Simonyan, J. S. Song, P. A. Thiessen, S. Vasudevan, Y. Wang, R. A. Yamashita, J. J. Yin, and S. H. Bryant.** 2003. CDD: a curated Entrez database of conserved domain alignments. Nucleic Acids Res. **31:**383–387.
41. **Matusan, A. E., M. J. Pryor, A. D. Davidson, and P. J. Wright.** 2001. Mutagenesis of the dengue virus type 2 NS3 protein within and outside helicase motifs: effects on enzyme activity and virus replication. J. Virol. **75:**9633–9643.
42. **Mise, K., and P. Ahlquist.** 1995. Host-specificity restriction by bromovirus cell-to-cell movement protein occurs after initial cell-to-cell spread of infection in nonhost plants. Virology **206:**276–286.
43. **Moore, S. D., and P. E. Prevelige, Jr.** 2002. A P22 scaffold protein mutation increases the robustness of head assembly in the presence of excess portal protein. J. Virol. **76:**10245–10255.
44. **Noueiry, A. O., J. Diez, S. P. Falk, J. Chen, and P. Ahlquist.** 2003. Yeast Lsm1p-7p/Pat1p deadenylation-dependent mRNA-decapping factors are required for brome mosaic virus genomic RNA translation. Mol. Cell. Biol. **23:**4094–4106.
45. **O'Reilly, E. K., N. Tang, P. Ahlquist, and C. C. Kao.** 1995. Biochemical and genetic analyses of the interaction between the helicase-like and polymerase-like proteins of the brome mosaic virus. Virology **214:**59–71.
46. **O'Reilly, E. K., Z. Wang, R. French, and C. C. Kao.** 1998. Interactions between the structural domains of the RNA replication proteins of plant-infecting RNA viruses. J. Virol.**72:**7160–7169.
47. **Pirttimaa, M. J., A. O. Paatero, M. J. Frilander, and D. H. Bamford.** 2002. Nonspecific nucleoside triphosphatase P4 of double-stranded RNA bacteriophage ϕ6 is required for single-stranded RNA packaging and transcription. J. Virol. **76:**10122–10127.
48. **Restrepo-Hartwig, M., and P. Ahlquist.** 1999. Brome mosaic virus RNA replication proteins 1a and 2a colocalize and 1a independently localizes on the yeast endoplasmic reticulum. J. Virol. **73:**10303–10309.
49. **Restrepo-Hartwig, M. A., and P. Ahlquist.** 1996. Brome mosaic virus helicase- and polymerase-like proteins colocalize on the endoplasmic reticulum at sites of viral RNA synthesis. J. Virol. **70:**8908–8916.
50. **Rikkonen, M., J. Peranen, and L. Kaariainen.** 1994. ATPase and GTPase activities associated with Semliki Forest virus nonstructural protein nsP2. J. Virol. **68:**5804–5810.
51. **Salonen, A., T. Ahola, and L. Kaariainen.** 2005. Viral RNA replication in association with cellular membranes. Curr. Top. Microbiol. Immunol. **285:** 139–173.
52. **Schwartz, M., J. Chen, M. Janda, M. Sullivan, J. den Boon, and P. Ahlquist.** 2002. A positive-strand RNA virus replication complex parallels form and function of retrovirus capsids. Mol. Cell **9:**505–514.
53. **Singleton, M. R., and D. B. Wigley.** 2002. Modularity and specialization in superfamily 1 and 2 helicases. J. Bacteriol. **184:**1819–1826.
54. **Sullivan, M. L., and P. Ahlquist.** 1999. A brome mosaic virus intergenic RNA3 replication signal functions with viral replication protein 1a to dramatically stabilize RNA in vivo. J. Virol. **73:**2622–2632.
55. **Tai, C. L., W. C. Pan, S. H. Liaw, U. C. Yang, L. H. Hwang, and D. S. Chen.** 2001. Structure-based mutational analysis of the hepatitis C virus NS3 helicase. J. Virol. **75:**8289–8297.
56. **Tanner, N. K., and P. Linder.** 2001. DExD/H box RNA helicases: from generic motors to specific dissociation functions. Mol. Cell **8:**251–262.
57. **Vasiljeva, L., A. Merits, P. Auvinen, and L. Kaariainen.** 2000. Identification of a novel function of the alphavirus capping apparatus. RNA 5′-triphosphatase activity of Nsp2. J. Biol. Chem. **275:**17281–17287.
58. **Velankar, S. S., P. Soultanas, M. S. Dillingham, H. S. Subramanya, and D. B. Wigley.** 1999. Crystal structures of complexes of PcrA DNA helicase with a DNA substrate indicate an inchworm mechanism. Cell **97:**75–84.
59. **Westaway, E., J. Mackenzie, M. Kenney, M. Jones, and A. Khromykh.** 1997. Ultrastructure of Kunjin virus-infected cells: colocalization of NS1 and NS3 with double-stranded RNA, and of NS2B with NS3, in virus-induced membrane structures. J. Virol. **71:**6650–6661.